THE JOURNAL OF PHYSICAL CHEMISTRY C

Article

pubs.acs.org/JPCC

Enhanced UV Response of Single Anodic TiO_2 Nanotube: Effect of Water-Modified Microstructures

Qiang Wang,*[,‡] Jun Jie Li,*[,†] and Chang Zhi Gu[†]

[†]Beijing National Laboratory for Condensed Matter Physics, Institute of Physics, Chinese Academy of Sciences, Beijing 100190, China

[‡]Department of Optics and Electronics Science, College of Science, Harbin Institute of Technology at Wei Hai, Weihai 264209, China

ABSTRACT: Water-modified ultraviolet (UV) light response of single anodic TiO_2 nanotube (NT) is reported in this article. After keeping in deionized water at room temperature, the original smooth surface of amorphous TiO_2 NTs is roughened and even changes into sponge-like structure by stacking of further oxidized and crystallized nanodots (NDs) through water-driven surface dissolution process. Two-dimensional variable range hopping (2D-VRH) model is recognized to interpret low-temperature electrical transport properties for the original NT, and the water-modified NT shows deviation from this mechanism owing to the additional electronic tunneling through the surface-crystallized NDs assemblies. The resistance in dark is increased about one order after water-modification due to surface carrier depletion by nanocontacts between crystalline NDs and the original amorphous core. The UV sensitivity S (I_{UV}/I_{dark}) of as-prepared single NT is ~1.6, and response and recovery times are about 0.39 and 0.45 s, respectively. S is increased to ~21.7 after surface water-modification, whereas response and recovery times are increased to 7.1 and 7.5 s, respectively. Surface water-modification will reduce the density of recombination centers and increase the trap state density of carriers in TiO_2 NT due to surface charge-separation effect, both leading to the larger UV sensitivity and response time. Single anodic TiO_2 NT shows no persistent photocurrent, and it can be applied as high-speed, high-sensitivity UV optoelectronic nanodevices.

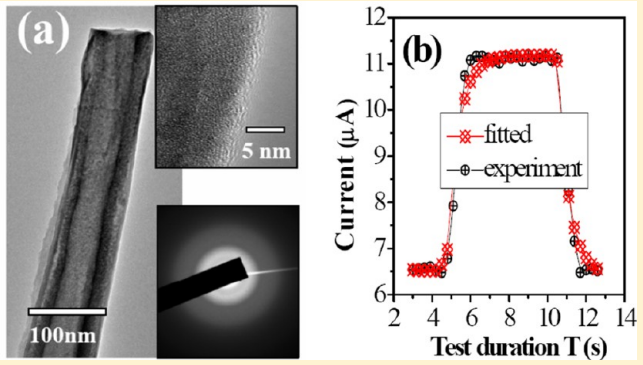

INTRODUCTION

Nanosized unit made from single low-dimensional nanostructure, such as nanowire (NW) or nanotube (NT), has drawn extensive concerns because a unique platform for fundamental investigations of nanosicence is provided. It can also be considered to be ideal building blocks for constructing versatile nanodevices due to the high surface-to-volume ratio and their special physical and chemical properties. TiO_2 NT array films formed by anodization of Ti foil have been intensively studied,[1] and they have attracted much attention because of both the unique microstructure and great prospects in photocatalyzing, biochemical sensing, and solar energy harvesting,[2−5] especially to note the pioneering work of Zwilling et al.[6] Ultraviolet (UV) light response is a remarkable property of anodic TiO_2, but it is confronted with such deficiencies as low responsibility, large response time, and persistent photocurrent. Recently UV nanodetectors formed by individual single-crystalline TiO_2 nanorod show smaller response time and higher responsibility than the amorphous counterparts,[7] and some applicable ways were reported to improve the UV photoelectricity conversion performances in low-dimensional amorphous TiO_2 nanostructures, among which TiO_2 nanostructures with surface-loading of plasmonic or catalytic nanoparticles (NPs) are suggested to be an efficient method.[8−10] Recently, spontaneous phase and morphology transformations of anodized amorphous titania NTs induced by water at room temperature have been studied,[11] which provides an unprecedented and promising way to apply anodic amorphous TiO_2 NTs as UV light sensor.

As far as we know, even though TiO_2 NT film is formed in water-containing electrolyte, the water post-treatment does not show significant effect on the properties of NTs film because it is formed by tightly bounded NTs and the water-dissolution reaction is not thorough. So far as well-isolated single NT is concerned, the water-modified effect should be much more prominent than the counterpart of bounded NTs in the film because it is very thoroughly exposed to water. Single TiO_2 NT measurements offer a unique way for probing individual and intrinsic behavior of TiO_2, which cannot be distinguished on the ensemble TiO_2 NT film, and in particular it can conveniently provide direct properties modification by water post-treatment to individual NT,[11] but well-dispersed single NT is not easy to get due to the friable mechanical properties of

Received: May 1, 2012
Revised: July 19, 2012
Published: July 24, 2012

   dx.doi.org/10.1021/jp304193z | J. Phys. Chem. C 2012, 116, 16864−16869

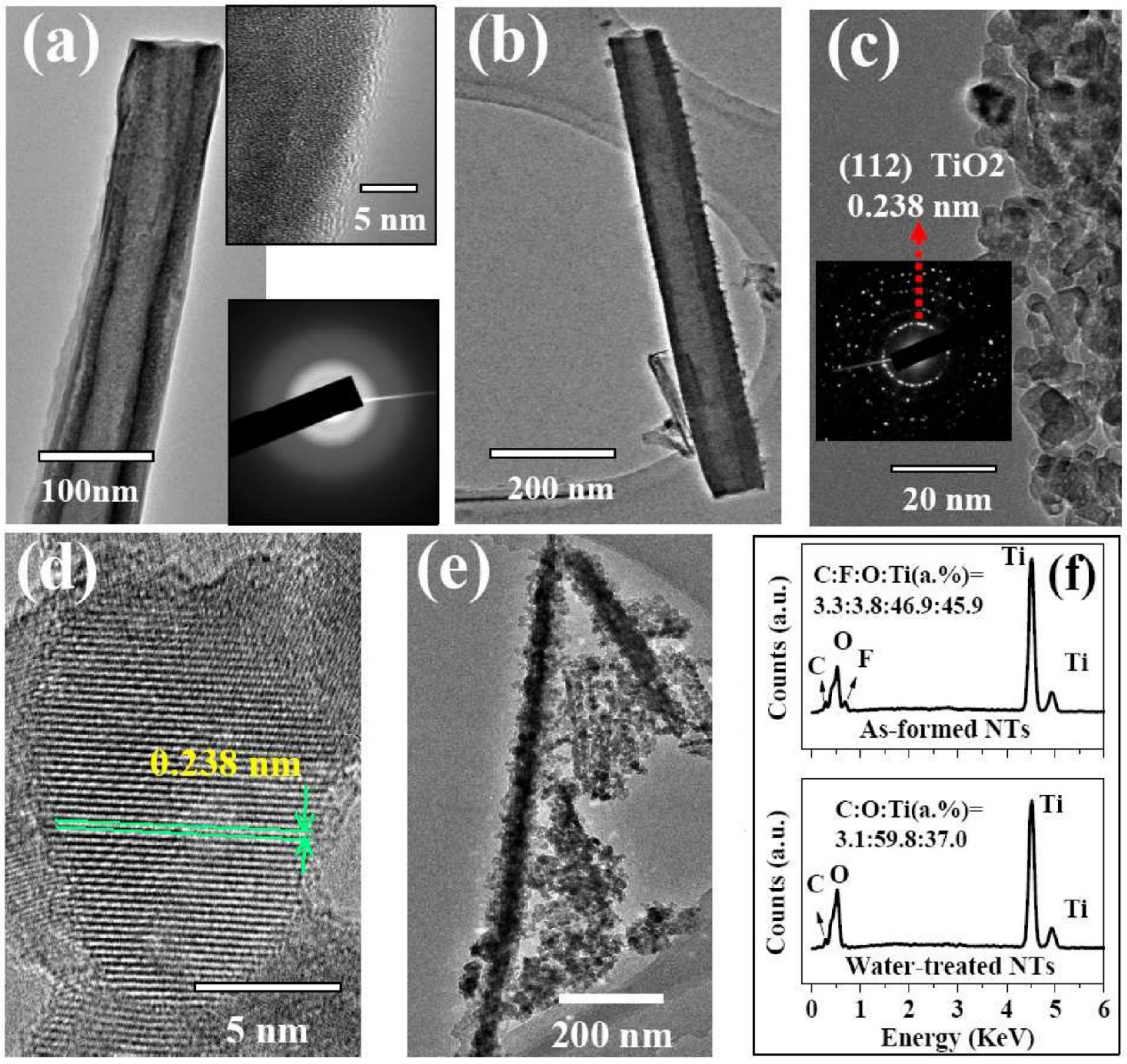

Figure 1. Microstructure characterizations of single TiO_2 NT. (a) TEM images of individual TiO_2 NT without water-modification inset with high-resolution image of the sidewall and electrons diffraction patterns. (b) TEM image of water-modified NT (72 h) showing roughened surface. (c) TEM image of the surface NDs inset with electrons diffraction pattern. (d) HRTEM image of one ND on the surface of water-modified NT (72 h). (e) TEM image of water-modified NTs (72 plus 72 h). (f) EDX spectra of TiO_2 NT (upper: as-formed NT, lower: water-modified NT).

TiO_2 NT film, and there are also difficulties in electrical measurement of individual NT with rather high resistivity, and hence its electronic transport property is scarcely reported so far.[12]

Here we report the electronic transport properties of single well-dispersed anodic TiO_2 NT with relatively low resistance due to Ohmic contact, and key points on its UV light response are emphasized to elucidate the effect of modified surface microstructure by soaked water. It is also important to understand the dynamics for generation, recombination, and transport of UV-generated electron carriers in single TiO_2 NT unit, for sake of manufacturing high-speed, high-sensitivity optoelectronic nanodevices.

EXPERIMENTAL SECTION

Titania films composed of highly ordered hexagonally structured NTs were synthesized by anodization of high-purity Ti foil (99.995%) in water-containing electrolyte [NH_4F (0.45 wt %)+ethylene glycol [$(HOCH_2)_2$] (98 vol %)+H_2O], and electrolyte temperature is controlled below 50 °C by using water bath. It is working under potentiostatic mode in electrochemical reaction tank, with high-quality graphite slat (covered with gold foil to reduce carbon contamination to the electrolyte) as the cathode. It was shown in our previous publication that both the length and diameter of as-formed NTs are complicatedly related to applied direct current (DC) voltage and reaction duration during anodization of Ti foil.[13] For preparation of titania NTs film, the applied constant DC voltage is 60 V with nearly constant current density of ~20 mA/cm^2, the interelectrode distance is ~1.5 cm with directly facing electrode area of ~4 cm^2, and the anodization time is 24 h. The atomic counts ratio of O and Ti is usually checked by using energy-dispersive X-ray spectroscopy (EDX), scanning electron microscopy (SEM), and transmission electron microscopy (TEM) are employed to characterize the morphologies and microstructures of as-formed TiO_2 NTs. After peeling off from Ti substrate, TiO_2 NT films were then ultrasonically dispersed in ethanol to prepare well-isolated single NT (the NT without water modification) for further TEM characterization and the formation of four-terminal electrical contacts to individual NT. Considering the friable mechanical properties of TiO_2 NTs, the ultrasonic dispersion

dx.doi.org/10.1021/jp304193z | J. Phys. Chem. C 2012, 116, 16864−16869

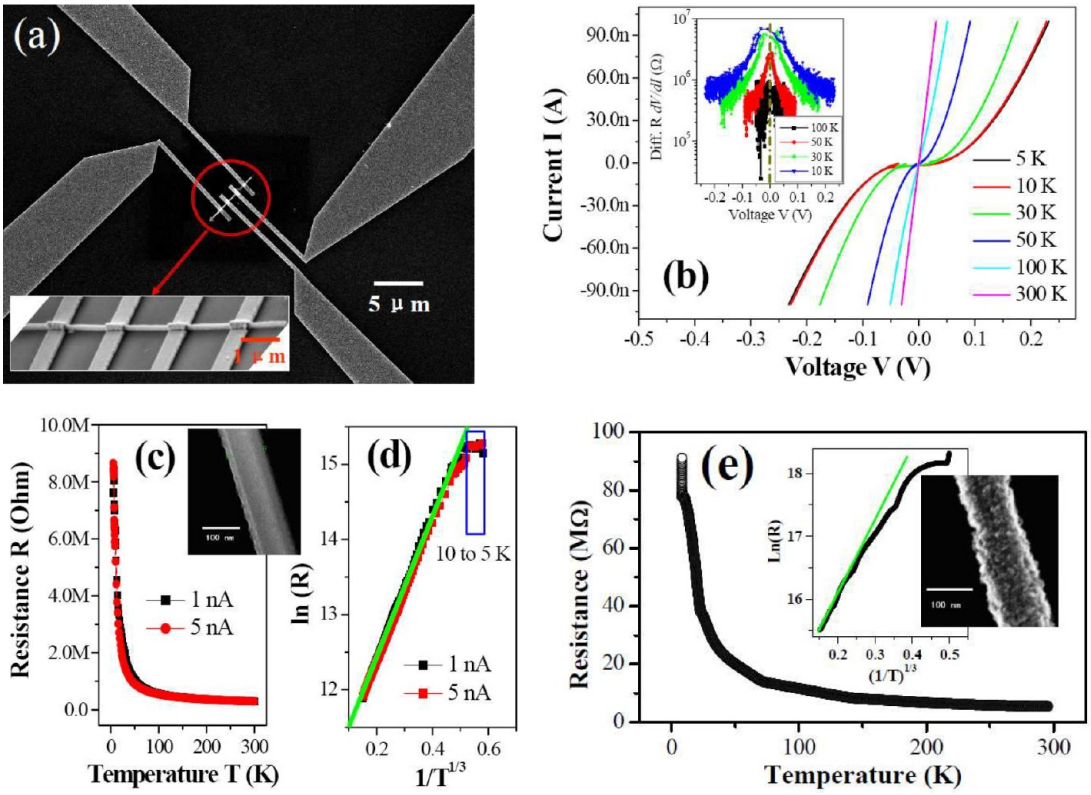

Figure 2. Electrical transport characterizations of single TiO_2 NT. (a) SEM images of single TiO_2 NT with four-terminal electrical contact configuration. (b) $I-V$ plots for NT without water-modification at different temperatures with inset of selected differential resistance dV/dI versus V plots. (c) $R-T$ plots at different driving currents for NT without water modification. (d) Fitted plots of ln $R(T)$ versus $(1/T)^{1/3}$ for NT without water modification. (e) $R-T$ plots for NT with water modification (72 h) inset with fitted plots of ln $R(T)$ versus $(1/T)^{1/3}$.

should be carried out at relatively low power with long duration of 1.5 to 2 h and single NT with length above 10 μm can be obtained. Just after dispersion, dipping, and drying, four-terminal electrical contacts onto individual NT were fabricated using a standard procedure of electron beam lithography (EBL, Reith 150), metallization, and lift-off. Magnetron-sputtering of 5 nm Ti film was followed by protective deposition of 100 nm Au film to form Ohmic-contact electrodes onto single TiO_2 NT. To obtain more reliable contacts to NT with large diameter, we performed further Pt remedy-deposition by using focused ion beam deposition (FIB, FEI DB235) for some contacts with crevices at the metal-semiconductor contacting position. After the original electrical measurements, as-fabricated TiO_2 NT nanounits were kept in deionized water in sealed plastic boxes for 72 h (or 72 plus 72 h) at room temperature to prepare water-modified single NT, and then the second electrical measurements in PPMS are carried out after long-time room-temperature nitrogen blow-drying.

Electrical transport measurements of single TiO_2 NT are performed using Physical Properties Measurement System (PPMS, Quantum Design) in the temperature range from 300 to 5 K. All electronic transport measurements in PPMS as well as the UV response measurements are performed by employing the four-terminal contact method. Low-frequency alternative current (AC) signals are used to obtain resistance versus temperature ($R-T$) dependence properties, and the high reproducibility of $R-T$ plots at different driving currents indicate that the thermoelectric effect is eliminated. The UV response measurements were performed in air at room temperature under steady-state illumination at 360 nm wavelength supplied by Xe arc lamp (with controllable electrical power from 200 to 500 W) with a monochromator. The resulting UV beam on the nanodevice unit had reached an approximate intensity of 0.6 mW/cm^2. The UV response of electrical current for single TiO_2 NT inside a closed black box with quartz optical window is documented by controlling the cyclic on/off states of UV illumination through a single-chip microcomputer. Because the resistance of TiO_2 NT is sensitive to the environmental humidity, NaCl saturated solution is added to the black box to set up stable humidity of 75.1% for UV response measurements.[13] Device currents at DC voltages were detected by using a pico-ampere-meter (Keithley 6487) connected to computer. The overall measurement setup is common-grounded and electrically screened form outer disturbance.

■ RESULTS AND DISCUSSION

The SEM characterizations of as-formed titania NTs film on Ti foil were shown in our previous publication.[13] Titania NTs, with pore size of ~50 nm and wall thickness of ~20 nm, are tightly bounded together. The TEM image with low resolution of single NT is shown in Figure 1a, inset with high-resolution TEM (HRTEM) image of the smooth sidewall and electrons diffraction pattern (blurred ring-like structure), indicating the amorphous microstructure of as-formed NTs. Microstructure of the water-modified NT (72 h) is shown in Figure 1b, showing many small protuberances, which is different to the smooth surface of as-formed NT shown in Figure 1a. TEM image of the sidewall for water-modified NT is shown in Figure 1c to exhibit many nanodots (NDs), and inset electrons diffraction pattern

dx.doi.org/10.1021/jp304193z | J. Phys. Chem. C 2012, 116, 16864−16869

shows superimposing of many types of patterns, indicating polycrystalline structure of TiO_2 with dominant orientation of (112). HRTEM image of the surface ND is shown in Figure 1d. It is well-crystallized NDs with size of ~5 nm and can be assigned to anatase TiO_2 (112) with lattice distance of 0.238 nm.[14] Figure 1e shows TEM image of water-modified NTs (72 h plus 72 h in deionized water at room temperature); the surface of NTs is severely deteriorated into sponge-like structures by stacking NDs.

The EDX spectra are shown in Figure 1f, and atomic ratio of Ti and O elements in as-formed NT exhibits excessive presence of Ti for the as-formed TiO_2 NTs. Interestingly, after keeping the TiO_2 NT in water for 72 h, more O is added (the atomic ratio is increased from 46.9 to 59.8%), whereas the atomic ratio of Ti and O is 37.0:59.8 (still below the stoichiometric ratio of 1:2 for standard crystalline TiO_2). Environmental and electrolyte contamination of carbon with rather low amount (below 3.5%) can be detected before and after water modification, but fluoride species is removed by the long-time water treatment, and they both do not disturb the atomic evaluation of Ti and O elements. Combining above characterizations, we think that surface water-modification will convert amorphous TiO_2 NT into further crystallized and oxidized states, whereas the original smooth surface will be changed to roughened and even sponge-like structures by stacking NDs. It was previously shown that TiO_2 NTs grown in ethylene glycol are contaminated with carbon and fluoride species,[15−17] and water-treatment cannot remove the carbon-enriched layer.[11] Our present result is in good agreement with these previous studies, whereas long-time water treatment can efficiently remove the fluoride species from titania NTs.

Four-terminal contact configuration for electrical transport study of single TiO_2 NT is shown in Figure 2a, whereas the lower left corner inset in Figure 2a shows the SEM image of four-terminal metallic contacts. As shown in Figure 2b, with the decrease in temperature from 300 to 5 K, the $I-V$ plots for the NT without water modification, documented by changing the driving AC current signals with low frequency of 0.3 Hz, first show linear $I-V$ dependence at 300 K (Ohmic contact properties), then begin to show more and more apparent symmetric nonlinear properties at lower temperatures (from 50 to 5 K). This rectifying effect is due to strong Columbic electron−electron interaction at low temperature[18,19] or field-induced phonon-tunneling effect.[20] As shown in inset plots of Figure 2b, the differential resistance, R_{diff}, is increased and more apparently voltage-dependent with the decrease in temperature, and it decreases with the increase in voltage drop (also indicating rectifying effect). To get rid of this effect, we intentionally study the plots of zero-bias resistance, R_0, for the NT without water modification (with inset SEM image) in dependence on temperature at different driving currents of 1 and 5 nA, respectively, which shows good reproducibility and elimination of thermoelectric effect, just as shown in Figure 2c. To discuss further the temperature-dependent intrinsic electrical properties, the dependence of $R_0(T)$ on T is fitted to obtain linear dependence of $\ln[R(T)]$ on $T^{-1/3}$ in the temperature region from 300 to 10 K. $R(T)$ is saturated and temperature-insensitive in the temperature region from 10 to 5 K, as shown in Figure 2d. A stable phase with no change in conductivity (from 10 to 5 K) indicates that electronic transport is due to electron transition in active defect states just about the Fermi level. Figure 2e shows the plot of zero-bias resistance, R_0, for the NT after water modification of 72 h (with inset SEM image) in dependence on temperature at driving currents of 5 nA, showing increased resistance (about one order) in comparison with that for NT without water modification, as shown in Figure 2c. For water-modified NT (72 h), it still shows linear $I-V$ plots at room temperature, indicating that the Ohmic contacts are intact. The inset plot of $\ln[R(T)]$ to $T^{-1/3}$ shows deviation to the linearity with very severe saturation (the experimental value is increasingly lower than the linearly fitted value) at low temperature (from 15 to 5 K). For the NT with further water modification (72 h plus 72 h), the original smooth surface has been dissolved into sponge-like structure, and no current can be detected (in both PPMS and UV response measurements) in this nanounit, which indicates electrical failure due to severely deteriorated contacts.

In disordered TiO_2 NT, there exists the possibility of electrons hopping (phonon-assisted tunneling) between local states in the vicinity of the Fermi level. The average hopping distance is increased with the increase in temperature, and it is named as variable range hopping (VRH) transport. For VRH transport, $\ln[R(T)]$ is proportional to $T^{-1/(d+1)}$, and d, being the hopping parameter, depends on the dimensionality of the system and the hopping distance.[21,22] The linear relation of $\ln[R(T)]$ versus $T^{-1/3}$ in Figure 2d well indicates that the VRH mechanism is applicable to interpret the electronic transport properties of individual TiO_2 NT in the temperature region from 300 to 10 K. The 2D ($d = 2$) VRH transport process is generally expressed by using Mott's conduction mode as[23]

$$R(T) = R_0 \exp\left[\left(\frac{T_0}{T}\right)^{1/3}\right] \quad (1)$$

where R_0 is a material parameter, temperature-independent T_0 is a temperature scale defined by electronic states density $N(E_F)$ at the Fermi level E_F, and T is the working temperature. For water-modified NT, the original amorphous phase is partially transformed into anatase phase by the surface water-modification, which indicates their electrical transport process should be different. In our present opinion, 2D VRH mechanism, defect-related transport, as well as electrons tunneling through surface NDs assemblies should all contribute to the overall complex electronic conducting process in water-modified TiO_2 NT, which introduces the deviation to the linearity at low temperature. At higher temperature, hopping conduction becomes the dominant mechanism, whereas a more profound and compressive interpretation is still under investigation.

As to the increased resistance for water-modified TiO_2 NT, a surface charge-depletion model is schematically proposed in Figure 3, in consideration of the contact potential between

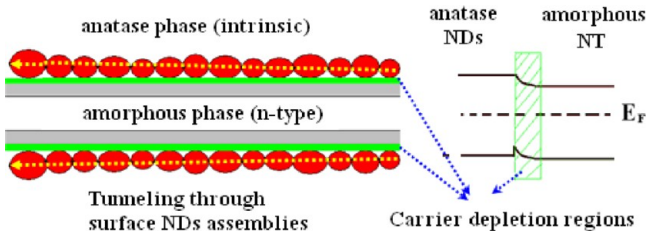

Figure 3. Schematic image for nanocontacts between crystallized NDs (intentionally enlarged) and amorphous core for water-modified NT (left part). The energy band diagram shows carrier depletion in the contacting positions (right part).

dx.doi.org/10.1021/jp304193z | J. Phys. Chem. C 2012, 116, 16864−16869

amorphous NT body and surface-crystallized anatase NDs. Because of the presence of band-tail states and oxygen vacancies, the original amorphous titania shows smaller band gap and n-type semiconducting properties.[24,25] After water modification, the water-driven dissolution–precipitation process will introduce the scraggy and even sponge-like surface,[11] and crystallized anatase NDs (with larger band gap and lower oxygen vacancy density as generally known) will contact the original amorphous titania core, resulting in upward band-bending and electron carrier depletion in the surface of water-modified TiO_2 NT, as shown in Figure 3. It will introduce a thinning effect of the conducting paths in the original NT, leading to the increased resistance. It should be pointed out that the increased dark resistance is not detrimental to the high UV sensitivity of the NT, just as shown in the following discussion.

Figure 4a shows the current versus time (I–t) characteristics for single NT without water modification at cyclic on/off states of UV illumination at different constant DC voltages. The UV sensitivity S (I_{uv}/I_{dark}) increases monotonically with applied DC voltage. Figure 4b shows the exponential decay fitting results of one specific cycle at constant DC voltages 2 V, and the response and recovery times for the as-prepared single TiO_2 NT are averagely as fast as 0.39 and 0.43 s, respectively. Figure 4c shows the UV response of single TiO_2 NT after water modification at 2 V, which shows greatly suppressed dark current of about one order (in good agreement with the transport results). The response and recovery times are on average 7.1 and 7.5 s, respectively, as can be seen from the fitted curves in Figure 4c. Fitting values show acceptable fitting error below 5% to the experimental results. It is worth mentioning that the response sensitivity S (I_{uv}/I_{dark}) of the NT without water modification is ~1.6, and it is increased to ~21.7 for the water-modified NT (72 h). It can be concluded that surface water-modification of TiO_2 NT can increase both the UV sensitivity and response time. As is well known, persistent photocurrent is detrimental to the performance of UV sensor, which implies that the photocurrent will not resume to the original dark value. This phenomenon is not observed for single NT before and after water modification, which indicates that single TiO_2 NT can be applied as high-speed, high-sensitivity UV optoelectronic nanodevices.

The long-lifetime carrier transport in metal oxide semiconductors UV sensor, such as TiO_2 and ZnO, is recently attributed to the oxygen-related photon-initiated chemical–physical reactions mechanism.[21] In the dark and oxygen-containing ambience, adsorption of foreign oxygen molecules creates electron trapping sites on the surface, leading to rather low conductivity. Under UV photoexcitation, electron–hole pairs are generated and separated by the surface built-in field, resulting in a longer lifetime τ and enhanced conductivity. Surface positively charged holes will release adsorbed oxygen species from the surface. Recombination could only take place, whereas oxygen molecules could readsorb on the surface. The lifetime τ of photon-excited carriers can efficiently change the value of current gain G and response time. The proportional relation between τ and G can be readily expressed as[26]

$$G \propto \frac{1}{L^2}\eta\tau\mu \qquad (2)$$

where η is the quantum efficiency for photoelectricity conversion, μ is the carrier mobility, and L is the interelectrode distance. As can be easily understood, the higher the photocurrent gain G, the larger the UV sensitivity S. τ will be large if the density of trap states in the forbidden band is large, and it will be small due to the presence of high density recombination centers. In our case, the small response and recovery times of individual amorphous TiO_2 NT are due to reduced lifetime τ of photoexcited carriers.[27] The suppression of τ also limits the attainable photocurrent gain G,[26] which is

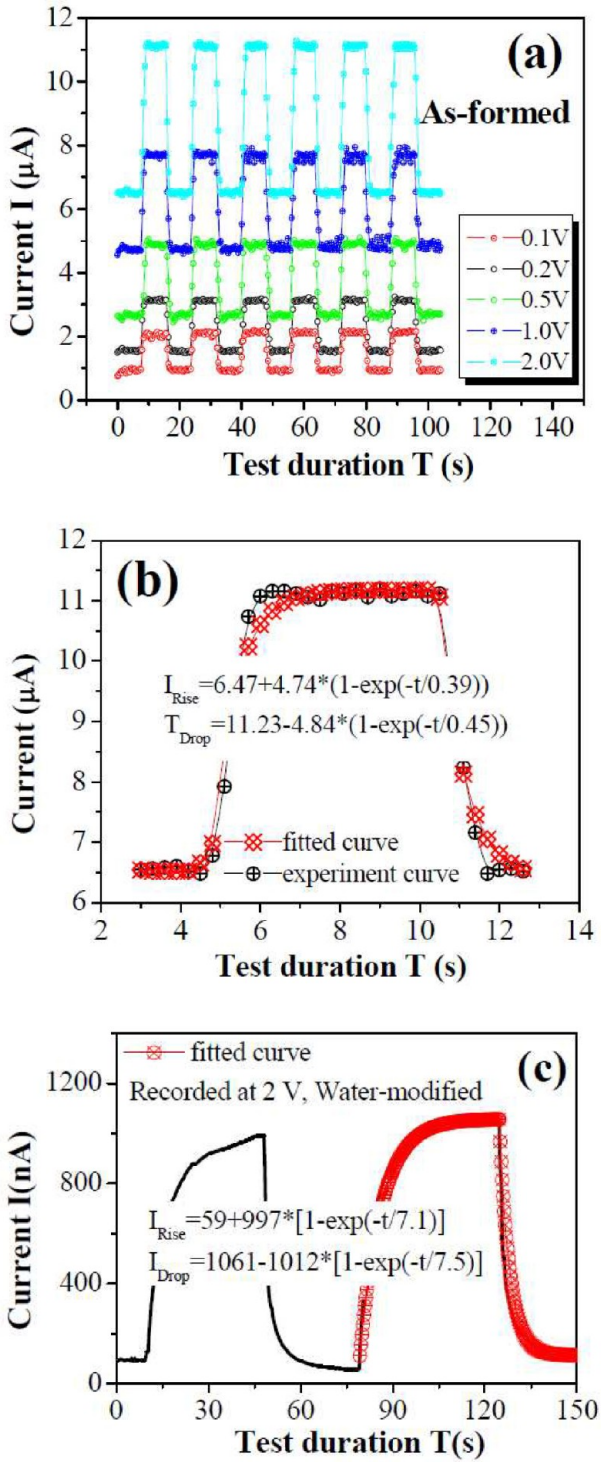

Figure 4. UV responses of single TiO_2 NT. (a) I–t plots of single as-prepared TiO_2 NT at different voltages. (b) Exponentially fitted I–t plots for single as-prepared TiO_2 NT. (c) I–t plots of TiO_2 NT after water modification with exponentially fitted results.

dx.doi.org/10.1021/jp304193z | J. Phys. Chem. C 2012, 116, 16864–16869

the number of photoelectrons generated by one photon. It is assumed that the transformation of amorphous phase to anatase phase for TiO_2 will proceed via a dissolution−precipitation process, in which randomly distributed $(TiO_6)^{2-}$ octahedra are dissolved and rearrange themselves driven by water and then precipitate as the anatase phase starts nucleating,[11] and the distinctive morphology transformation should be closely related to this water-driven dissolution−precipitation process. Further crystallization and oxidization of the original NT can reduce the density of recombination centers. Tunneling current through surface NDs assemblies had been previously verified in single TiO_2 nanofiber loaded with surface Au NDs.[8] Tunnel junctions in cascade nanostructures can provide adequate barriers to prevent carriers from leaking from one nanoregion efficiently by staying in trapped states while at the same time remain low in tunneling resistance for current recycling.[28] In our present case, surface water-modification can also increase the trap state density of carriers in TiO_2 NT due to carrier deposition in the cascaded tunneling junctions between surface NDs, just as schematically shown in Figure 3. The roughened surface by stacking of NDs should also be helpful for creating more trapping sites of oxygen species on the NT surface. As a result, lifetime τ of photoexcited carriers will be increased, which will result in the increased response and recovery times, and the UV sensitivity will also be increased resultantly. To fabricate perfect high-speed, high-sensitivity UV optoelectronic nanodevices, further research on TiO_2 NT should still be carried out to reduce the response time, in the meantime maintaining high sensitivity.

CONCLUSIONS

In conclusion, we have studied the electrical transport properties and UV responses of single TiO_2 NT. For designing of nanodevices for enhanced chemical sensing and harvesting of photons energy, the surface states usually play key role. The single as-formed TiO_2 NT exhibits fast UV response, whereas UV response is enhanced and slowed after water modification due to reduction of the density for surface recombination centers. Surface water-modification will increase the trap state density of carriers in TiO_2 NT due to carrier deposition in the cascaded tunneling junctions between surface NDs, leading to deviation of electronic transport properties away from the 2D VRH mechanism, which can also contribute to the increased UV response times and the response sensitivity S. Single anodic TiO_2 NT after water-modification shows on/off current ratio above 20 and response/recovery times of several seconds, and no persistent photocurrent phenomenon is detected, which indicates that it can be applied as high-speed, high-sensitivity UV optoelectronic nanodevices.

AUTHOR INFORMATION

Corresponding Author

*E-mail: wq19750505@tom.com (Q.W.); jjli@aphy.iphy.ac.cn (J.J.L.).

Notes

The authors declare no competing financial interest.

ACKNOWLEDGMENTS

This work was financially supported by the National Natural Science Foundation of China (nos. 60907023, 50825206, and 91023041) and the Knowledge Innovation Project of CAS (grant no. KJCX2-EW-W02). We are also thankful to the financial support of Shandong Excellent Young Scientist Research Award Fund Project (no. BS2011CL002). We show special thanks to financial support for Innovation Project of Harbin Institution of Technology.

REFERENCES

(1) Roy, P.; Berger, S.; Schmuki, P. *Chem. Int. Ed.* **2011**, *50*, 2904−2939.
(2) Grätzel, M. *Nature* **2001**, *414*, 338−344.
(3) Bach, U; Lupo, D.; Comte, P.; Moser, J. E. F.; Weissörtel, Salbeck, J.; Spreitzer, H.; Grätzel, M. *Nature* **1998**, *395*, 583−585.
(4) Xie, X. N.; Xie, Y. L.; Gao, X. Y.; Sow, C. H.; Andrew, T. S. W. *Adv. Mater.* **2009**, *21*, 3016−3021.
(5) Zheng, Q.; Zhou, B.; Bai, J. *Adv. Mater.* **2008**, *20*, 1044−1049.
(6) Zwilling, V.; Darque-Ceretti, E.; Boutry-Forveille, A.; David, D.; Perrin, M. Y.; Aucouturier, M. *Surf. Interface Anal.* **1999**, *27*, 629−637.
(7) Chen, R. S.; Chen, C. A.; Tsai, H. Y.; Wang, W. C.; Huang, Y. S. *Appl. Phys. Lett.* **2012**, *100*, 123108.
(8) Son, M. S.; Im, J. E.; Wang, K. K.; Oh, S. L.; Kim, Y. R.; Yoo, K. H. *Appl. Phys. Lett.* **2010**, *96*, 023115.
(9) Syed, M.; Gerardo, H.; Daniel, M. *Nano Lett.* **2011**, *11*, 5548−5552.
(10) Sri, P. S.; Nathaniel, K. G.; Nikolay, M.; Naomi, J. H. *Nano Lett.* **2008**, *8*, 624−630.
(11) Wang, D.; Liu, L.; Zhang, F.; Tao, K.; Pippel, E.; Domen, K. *Nano Lett.* **2011**, *11*, 3649−3655.
(12) Fabrega, C.; Francisco, H.; Prades, J. D.; Roman, J.; Andreu, T.; Morante, J. R. *Nanotechnology* **2010**, *21*, 445703−445708.
(13) Wang, Q.; Pan, Y. Z.; Huang, S. S.; Ren, S. T.; Li, P.; Li, J. J. *Nanotechnology* **2011**, *22*, 025501−025512.
(14) Chen, Z.; Dawson, G.; Liu, J.; Dai, K. *Micro Nano Lett.* **2011**, *6*, 675−677.
(15) Albu, S. P.; Ghicov, A.; Aldabergenova, S.; Drechsel, P.; LeClere, D.; Thompson, G. E.; Macak, J. M.; Schmuki, P. *Adv. Mater.* **2008**, *20*, 4135−4139.
(16) Berger, S.; Albu, S. P.; Schmidt-Stein, F.; Hilderbrand, H.; Schmuki, P.; Hammond, J. S.; Paul, D. F.; Reichlmaier, S. *Surf. Sci.* **2011**, *605*, L57−60.
(17) Ji, Y.; Lin, K. C.; Zheng, H.; Zhu, J. J.; Samia, A. C. S. *Electrochem. Commun.* **2011**, *13*, 1013−1015.
(18) Ma, Y. J.; Zhang, Z.; Zhou, F.; Lu, L.; Jin, A. Z.; Gu, C. Z. *Nanotechnology* **2005**, *16*, 746−750.
(19) Sandow, B.; Gloos, K.; Rentzsch, R.; Ionov, A. N.; Schirmacher, W. *Phys. Rev. Lett.* **2001**, *86*, 1845−1848.
(20) Pipinys, P.; Kiveris, A. *Physica B* **2008**, *403*, 3730−3733.
(21) Ma, Y. J.; Zhou, F.; Lu, L.; Zhang, Z. *Solid State Commun.* **2004**, *130*, 313−316.
(22) Zhao, Y. L.; Lv, W. M.; Liu, Z. Q.; Zeng, S. W.; Motapothula, M.; Dhar, S.; Ariando, K.; Wang, Q.; Venkatesan, T. *AIP Adv.* **2012**, *2*, 012129.
(23) Lin, Y. F.; Chen, T. H.; Chang, C. H.; Chang, Y. W.; Chiu, Y. C.; Hung, H. C.; Kai, J. J.; Liu, Z. P.; Fang, J. Y.; Jian, W. B. *Phys. Chem. Chem. Phys.* **2010**, *12*, 10928−10933.
(24) Jeong, H. Y.; Lee, J. Y.; Choi, S. Y. *Appl. Phys. Lett.* **2010**, *97*, 042109.
(25) Cho, E.; Han, S. *Phys. Rev. B* **2006**, *73*, 193202−193205.
(26) Ren, S. T.; Wang, Q.; Zhao, F.; Qu, S. L. *Chin. Phys. B* **2012**, *21*, 038104−038111.
(27) Kroeze, J. E.; Savenije, T. J.; Warman, J. M. *J. Am. Chem. Soc.* **2004**, *126*, 7608−7618.
(28) Murray, L. M.; Norton, D. T.; Olesberg, J. T.; Boggess, T. F.; Prineas, J. P. *J. Vac. Sci. Technol., B* **2012**, *30*, 021203−021209.